

Investigations of two trigonal (T_1 and T_2) Gd^{3+} ESR centers in treated alkaline-earth-fluoride crystals*

Chi-Chung Yang,[†] Sook Lee, and Albert J. Bevelo[‡]

Department of Physics, Saint Louis University, St. Louis, Missouri 63103

(Received 28 May 1975)

A detailed investigation has been made of the two trigonal Gd^{3+} ESR centers (T_1 and T_2) in alkaline-earth-fluoride (CaF_2 , SrF_2 , and BaF_2) crystals treated with water vapor at high temperatures. We have observed both the T_1 and T_2 centers in all three fluoride crystals. Partially resolved superhyperfine structures have been detected for the first time for the T_1 and T_2 centers. It is established that the charge-compensation structures of the T_1 and T_2 trigonal Gd^{3+} centers are associated with the $Gd^{3+} - F^-O_4^{2-}$ and $Gd^{3+} - F_7^-O_2^-$ configurations, respectively.

I. INTRODUCTION

It was first observed by Sierro^{1,2} that heat treatment of CaF_2 crystals with water vapor at high temperatures resulted in the disappearance of the original cubic³⁻⁷ and tetragonal^{2,8-11} Gd^{3+} ESR centers in the crystals and produced two new types of trigonally symmetric Gd^{3+} centers. One of these trigonal centers is associated with a relatively small axial fine-structure splitting characterized by $b_2^0 \approx -407 \times 10^{-4} \text{ cm}^{-1}$, and the other trigonal center is associated with a rather large value of $b_2^0 \approx -1667 \times 10^{-4} \text{ cm}^{-1}$. Throughout this paper, the former center is referred to as the T_1 , and the latter as the T_2 trigonal Gd^{3+} centers. Sierro^{2,12} also observed the T_2 -type center in treated SrF_2 but not the T_1 -type center; neither center was observed in BaF_2 . Sierro¹ proposed that the T_1 and T_2 centers involved an OH^- and an O^{2-} ion, respectively, each of which replaces one of the eight nearest-neighbor F^- ions surrounding the Gd^{3+} ion ($Gd^{3+} - F_8^-$) in the fluorite lattice.

Sierro's model for the T_1 center was later disputed by Gil'fanov, Livanova, and Stolov.¹³ They pointed out that the substitution of an OH^- ion for an F^- ion in the $Gd^{3+} - F_8^-$ configuration did not provide the extra negative charge necessary for compensating the Gd^{3+} ion at the divalent Ca^{2+} site in CaF_2 . They suggested instead that the OH^- ion should be located at an interstitial position along the $[111]$ direction next to the Gd^{3+} ion. Vinokurov *et al.*¹¹ made further studies of the T_2 -type Gd^{3+} center in CaF_2 and obtained improved values for the spin-Hamiltonian constants for this center.

In this paper, we report the results of our ESR investigations of a series of treated crystals of CaF_2 , SrF_2 , and BaF_2 containing dilute amounts of Gd^{3+} ions. We have observed for the first time the T_1 -type center in SrF_2 and both the T_1 - and T_2 -type centers in BaF_2 , thus completing the observation of these two trigonal Gd^{3+} centers in all three alkaline-earth-fluoride systems.¹⁴ The observed

ESR fine-structure spectra have been quantitatively analyzed, resulting in a complete determination of their spin-Hamiltonian constants. We have also detected partially resolved superhyperfine structures for the T_1 and T_2 Gd^{3+} centers, from which we have concluded that the charge-compensation models for these two trigonal Gd^{3+} centers are similar to those established previously^{15,16} for the two trigonal Yb^{3+} and Ce^{3+} ESR centers produced in treated CaF_2 .

II. EXPERIMENTAL

A. Sample preparation

The alkaline-earth-fluoride crystals investigated in the present work were obtained from Optovac, Inc. The crystals are designated according to their nominal wt. % Gd^{3+} - ion concentrations as $CaF_2:10^{-4}\%$ Gd^{3+} , $CaF_2:10^{-3}\%$ Gd^{3+} , $CaF_2:5 \times 10^{-2}\%$ Gd^{3+} , $SrF_2:10^{-4}\%$ Gd^{3+} , $SrF_2:10^{-3}\%$ Gd^{3+} , $SrF_2:5 \times 10^{-2}\%$ Gd^{3+} , $BaF_2:10^{-4}\%$ Gd^{3+} , $BaF_2:10^{-3}\%$ Gd^{3+} , and $BaF_2:5 \times 10^{-2}\%$ Gd^{3+} .

Heat treatment of the samples was performed in a vacuum system consisting of a glass bell jar with a brass base plate, a fore pump, a diffusion pump, and a liquid-nitrogen cold trap. Two semicircular heating elements were used to form an oven capable of reaching 1200 °C. A glass vessel with a narrow neck containing a stop cock was connected through the base plate for introducing water vapor into the vacuum chamber. The water vapor pressure inside the system was measured by a pressure gauge covering the range from 1 to 1000 mTorr, and the oven temperature was monitored by a chromel-alumel thermocouple near the sample.

Samples with a typical size of $0.3 \times 0.3 \times 0.6 \text{ cm}^3$ were placed in a ceramic crucible which was completely filled with fine CaF_2 powders in order to avoid excessive reaction of the water vapor with the samples. This method was very effective in retarding the hydrolysis reaction thus enabling us to analyze systematically the production of the T_1

and T_2 centers.

A typical sample-preparation experiment was performed in the following manner. The bell jar system was first outgassed at 1200 °C for 24 h to remove any water vapor from the system. After placing the sample, the system was again outgassed at 400 °C for 10 h. The temperature was then raised to the desired treatment temperature (usually near 1000 °C) over a period of several hours. After the sample was isolated from the pumping system, a given amount of water vapor (usually several hundred mTorr) was introduced into the bell jar. The sample was maintained at the treatment temperature for a specific period of time (usually several hours) before the oven was shut off allowing the sample to cool to room temperature for ESR experiments.

B. Fine-structure investigations

The ESR experiments were performed using a Varian V-4500 X-band ESR spectrometer operating at a microwave frequency of approximately 9.5 GHz at room temperature and 9.2 GHz at 77 °K. The spectrometer system employs a 100-kHz field modulation and a Varian 12-in. electromagnet with a field-regulated power supply.

Before treatment, the $\text{CaF}_2:10^{-4}\%$ Gd^{3+} sample exhibited primarily the tetragonal^{2,8-11} Gd^{3+} ESR center and a trace of the cubic³⁻⁷ Gd^{3+} center. Treating the sample at 900 °C for 4 h at a water vapor pressure of 400 mTorr resulted in a disappearance of the original tetragonal and cubic Gd^{3+} centers, and produced a different set of ESR lines. These ESR lines were identified as those arising from a trigonal Gd^{3+} center with an axial fine-structure splitting constant $b_2^0 \approx -1668 \times 10^{-4} \text{ cm}^{-1}$, which is the T_2 -type center observed in CaF_2 by Sierro. When another $\text{CaF}_2:10^{-4}\%$ Gd^{3+} sample was treated under the same conditions but at a different water vapor pressure of 1000 mTorr, the original tetragonal and cubic Gd^{3+} centers were found to be converted to another trigonal Gd^{3+} center having $b_2^0 \approx -409 \times 10^{-4} \text{ cm}^{-1}$, which is the T_1 -type center observed in CaF_2 by Sierro.

Although the observation of the T_1 and T_2 trigonal Gd^{3+} ESR centers in the heat-treated $\text{CaF}_2:10^{-4}\%$ Gd^{3+} sample as well as the fine-structure splittings associated with these two centers were consistent with the previous work by Sierro,^{1,2} the sequence of appearance for these two centers required further studies. We thus performed a series of heat-treatment experiments in the $\text{CaF}_2:10^{-3}\%$ Gd^{3+} and $\text{CaF}_2:5 \times 10^{-2}\%$ Gd^{3+} samples by fixing the treatment temperature and water vapor pressure and studying the production of the T_1 and T_2 centers as a function of time. Because of the higher Gd^{3+} concentrations in these crystals, the conversion of the original Gd^{3+} centers to the T_1 and T_2 centers was slow-

er and hence easier to examine. These experiments revealed that the T_2 center was always produced in the initial stage of the hydrolysis reaction just as the original tetragonal and cubic Gd^{3+} centers began to decrease in intensity. When the same sample was further treated, the T_1 center appeared. It should be pointed out that, although the final amount of the T_1 and T_2 centers produced in a given treatment as well as their relative intensities depended upon the treatment conditions, the production sequence of these two centers was always the same; that is, T_2 followed by T_1 . This sequence was just the opposite of that suggested by Sierro in treated CaF_2 .

Heat treatment of SrF_2 was first performed in the $\text{SrF}_2:10^{-4}\%$ Gd^{3+} sample. Prior to treatment, this sample contained approximately 60% tetragonal^{2,12} and 40% weak trigonal^{2,12} Gd^{3+} centers with a trace of the cubic^{2,12} Gd^{3+} center. After treating the sample at 900 °C for 5 h at a water vapor pressure of 400 mTorr, the original Gd^{3+} ESR lines disappeared completely, while a new set of ESR lines arose. These ESR lines are shown in Fig. 1 for \vec{H} parallel to the [111], [110], and [100] directions. The labelling S, D, T, or Q designates, re-

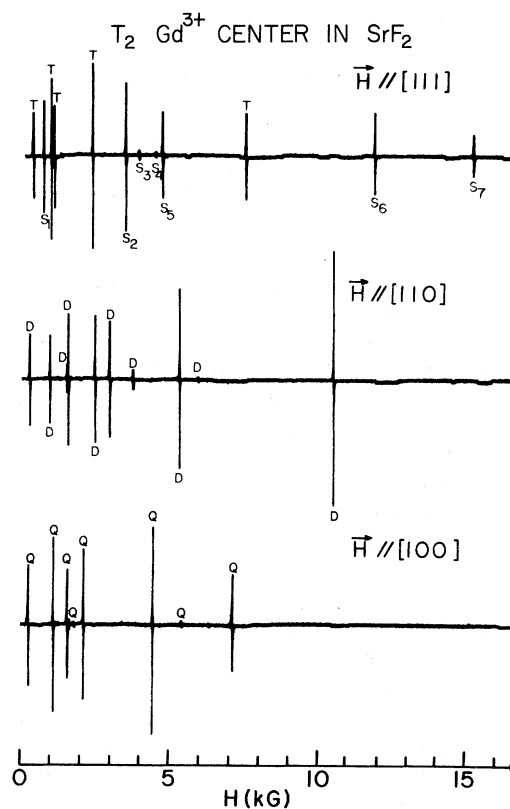


FIG. 1. ESR fine-structure spectra of the T_2 trigonal Gd^{3+} center in treated $\text{SrF}_2:10^{-4} \text{ Gd}^{3+}$ at room temperature.

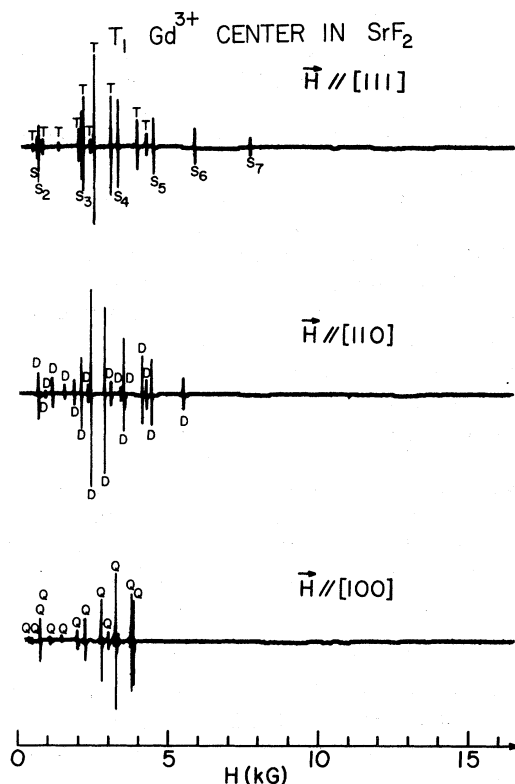


FIG. 2. ESR fine-structure spectra of the T_1 trigonal Gd^{3+} center in treated $SrF_2:10^{-4}\%$ Gd^{3+} at room temperature.

spectively, singlet, doublet, triplet, or quartet line, referring to the number of transitions that each fine-structure line contains.¹⁷ We have found that these ESR lines arise from a trigonal Gd^{3+} center with $b_2^0 \approx -1816 \times 10^{-4} \text{ cm}^{-1}$, which is consistent with the T_2 -type center observed in SrF_2 by Sierro.^{2,12}

When another $SrF_2:10^{-4}\%$ Gd^{3+} sample was treated under the same conditions but at an increased water vapor pressure of 1000 mTorr, the resultant ESR spectra displayed an entirely new set of trigonal Gd^{3+} ESR lines. The ESR spectra are shown in Fig. 2 for the three crystallographic axes. These ESR lines are characterized by an axial fine-structure splitting constant b_2^0 of roughly $-615 \times 10^{-4} \text{ cm}^{-1}$, indicating the first observation of the T_1 -type Gd^{3+} center in SrF_2 .

Having successfully produced the T_1 -type center in SrF_2 , we then attempted to produce the T_1 - and T_2 -type centers in BaF_2 . Initially the $BaF_2:10^{-4}\%$ Gd^{3+} sample contained primarily the weak trigonal^{2,12,18,19} Gd^{3+} center and some very weak signals from the cubic^{2,12,19,20} Gd^{3+} center. Treatment of the sample at 850 °C for 5 h at a water vapor pressure of 300 mTorr completely removed the origi-

nal Gd^{3+} ESR lines, and produced a new set of ESR lines shown in Fig. 3. Analyses of these ESR lines revealed that they were associated with a trigonal Gd^{3+} center having $b_2^0 \approx -1700 \times 10^{-4} \text{ cm}^{-1}$, corresponding to the T_2 type trigonal Gd^{3+} center. The production of the T_1 -type center in BaF_2 was achieved by treating another $BaF_2:10^{-4}\%$ Gd^{3+} sample under the same conditions but at a water vapor pressure of 1000 mTorr. The resultant ESR spectra are shown in Fig. 4. This center is characterized by $b_2^0 \approx -899 \times 10^{-4} \text{ cm}^{-1}$.

The production sequence of the T_1 and T_2 centers in the SrF_2 and BaF_2 crystals containing $10^{-3}\%$ and $5 \times 10^{-2}\%$ Gd^{3+} ions was also examined. In all cases, it was found that the T_2 center was produced before the T_1 center in the heat-treatment experiments, the same sequence as we observed in CaF_2 .

C. Superhyperfine-structure observations

No superhyperfine structure has been reported in the previous investigations of the T_1 and T_2 centers.^{1,2,11-14,21} Based on our experience²² in detecting superhyperfine structures for the cubic Gd^{3+} center in CaF_2 , SrF_2 , and BaF_2 , however, we have observed some partially resolved superhyperfine

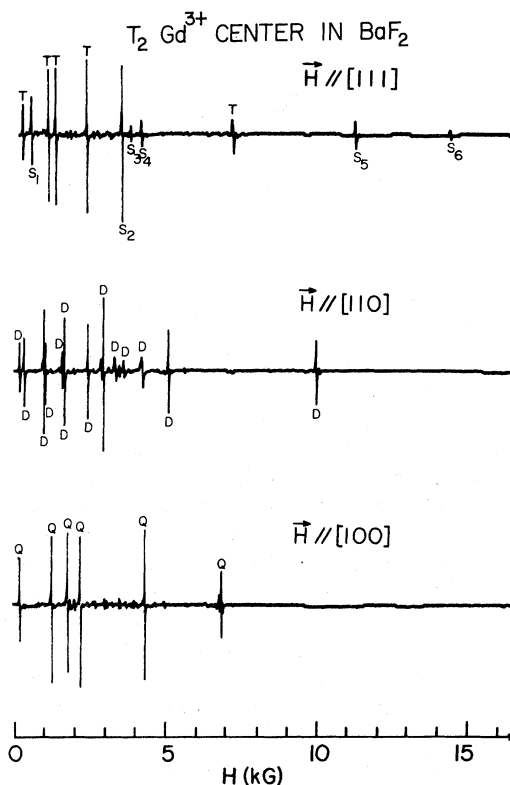


FIG. 3. ESR fine-structure spectra of the T_2 trigonal Gd^{3+} center in treated $BaF_2:10^{-4}\%$ Gd^{3+} at room temperature.

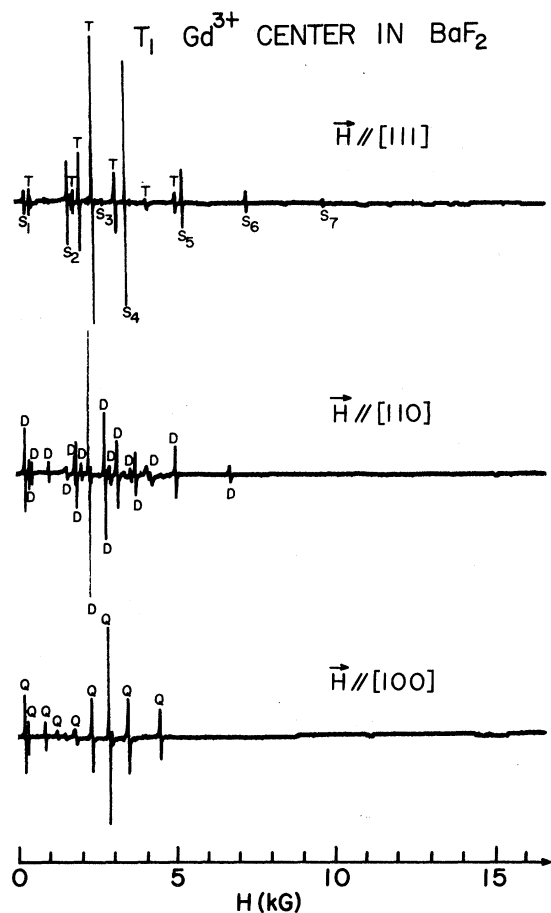


FIG. 4. ESR fine-structure spectra of the T_1 trigonal Gd^{3+} center in treated $BaF_2:10^{-4}\%$ Gd^{3+} at room temperature.

structures for both the T_1 and T_2 centers in the three fluoride crystals at 77 °K.

For the T_1 center in the $SrF_2:10^{-3}\%$ Gd^{3+} sample, when the external magnetic field \vec{H} was applied along the [111] direction of the crystal, each of the seven singlet fine-structure lines indicated by S_1 to S_7 in Fig. 2 displayed a doublet superhyperfine structure with weak satellite lines. The structure is shown in Fig. 5. It is noted that each component line in the doublet structure has a linewidth of roughly 2 G for all seven fine-structure lines. As the magnetic field \vec{H} was rotated away from the [111] direction, the doublet structure became less resolved and eventually not detectable. No superhyperfine structure was observed for any other fine-structure line when \vec{H} was in the vicinity of the [110] or [100] axis. A similar doublet structure was also observed for the T_1 center in the $CaF_2:10^{-3}\%$ Gd^{3+} and $BaF_2:10^{-3}\%$ Gd^{3+} samples, except that the resolution of the doublet structure was slightly poorer in CaF_2 and poorest in BaF_2 .

A similar doublet superhyperfine structure was observed for the T_1 center in the CaF_2 , SrF_2 , and BaF_2 crystals containing $10^{-4}\%$ Gd^{3+} ions. On the other hand, the samples containing $5 \times 10^{-2}\%$ Gd^{3+} ions displayed the doublet structure with very poor resolution.

For the T_2 center in $SrF_2:10^{-3}\%$ Gd^{3+} sample, only one fine-structure line indicated by S_2 in Fig. 1 for $\vec{H} \parallel [111]$ exhibited a partially resolved multiplet superhyperfine structure. The structure is shown in Fig. 6. It is noted that this structure has a central line and contains at least nine components. The remaining fine-structure transitions had linewidths of roughly 10 G and exhibited no resolved superhyperfine structure. In the $CaF_2:10^{-3}\%$ Gd^{3+} and $BaF_2:10^{-3}\%$ Gd^{3+} samples, a similar superhyperfine structure with poorer resolution was observed for the S_2 fine-structure line. The CaF_2 , SrF_2 , and BaF_2 crystals containing $5 \times 10^{-2}\%$ Gd^{3+} ions showed no resolved superhyperfine structure for the T_2 center.

D. Treatment with D_2O vapor

The alkaline-earth-fluoride crystals containing $10^{-4}\%$, $10^{-3}\%$, and $5 \times 10^{-2}\%$ Gd^{3+} ions were also treated with D_2O vapor. In these crystals, no dif-

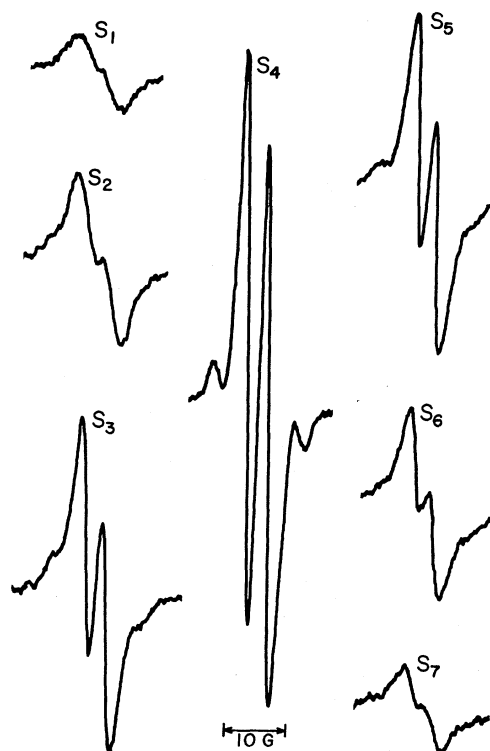


FIG. 5. Doublet superhyperfine structure observed for the seven singlet (S) fine-structure lines of the T_1 trigonal Gd^{3+} center for $\vec{H} \parallel [111]$ in $SrF_2:10^{-3}\%$ Gd^{3+} at 77 °K.

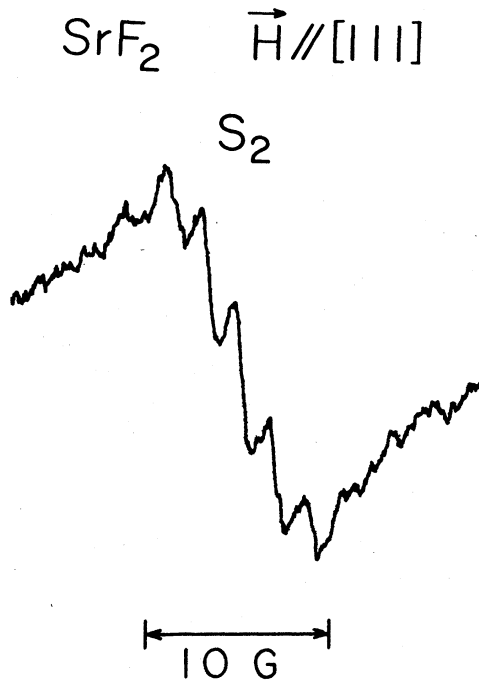


FIG. 6. Superhyperfine structure observed for the S_2 singlet fine-structure line of the T_2 trigonal Gd^{3+} center for $\vec{H} \parallel [111]$ in $SrF_2 : 10^{-3}\% Gd^{3+}$ at 77°K.

ference was observed for either the fine structure or the superhyperfine structure as compared to crystals treated with H_2O vapor.

III. ANALYSES AND DISCUSSIONS

A general description has been given elsewhere¹⁷ for the study of the ESR fine-structure properties of the $^8S_{7/2}$ ground state of Gd^{3+} under the influence

of a trigonally symmetric crystalline environment. It is convenient to characterize these ESR properties by the following spin Hamiltonian²¹:

$$\mathcal{H} = g\mu_B \vec{H} \cdot \vec{S} + \frac{1}{3}b_2^0 O_2^0 + \frac{1}{60}(b_4^0 O_4^0 + b_4^3 O_4^3) + \frac{1}{1280}(b_6^0 O_6^0 + b_6^3 O_6^3 + b_6^6 O_6^6). \quad (1)$$

In order to determine the spin-Hamiltonian constants for the T_1 and T_2 centers, we have employed an iterative computer program¹⁷ to diagonalize numerically the entire spin-Hamiltonian matrix and fit the theoretical spectra to the experimental data. The best-fit values obtained by least-squares method are listed in Table I. It is noted that our values for the T_1 and T_2 centers in CaF_2 and the T_2 center in SrF_2 are in agreement with those obtained previously by Sierro² and by Vinokurov *et al.*¹¹

Sierro's assignment of an OH^- ion for the T_1 center and an O^{2-} ion for the T_2 center was based on the following considerations.¹ At the beginning of the hydrolysis reaction, water molecules were considered to be dissociated into H^+ and OH^- ions. The H^+ ion combined with F^- ions to form HF acid, while the OH^- ion took the place of the removed F^- ion in the first shell, resulting in the T_1 center. As the hydrolysis treatment was continued, the hydrogen was removed from the OH^- ion leaving an O^{2-} ion in the first shell, resulting in the T_2 center. It is believed that Sierro's models may have been partly based on his observation that the T_1 center was produced before the T_2 center in the hydrolysis treatment. Gil'fanov *et al.*¹³ later proposed that an OH^- ion should be located at an interstitial position along the $[111]$ direction adjacent to the Gd^{3+} ion in order to accomplish the required charge compensation.

TABLE I. Spin-Hamiltonian constants for the T_1 and T_2 trigonal Gd^{3+} centers in CaF_2 , SrF_2 , and BaF_2 at room temperature, where b_n^m are given in units of 10^{-4} cm^{-1} .

	g	b_2^0	b_4^0	b_6^0	b_4^3	b_6^3	b_6^6
T_1 in CaF_2	1.9910 ± 0.0004	-409.3 ± 0.2	-13.9 ± 0.1	-0.1 ± 0.1	+230 ± 2	-8 ± 3	-6 ± 2
T_1 in SrF_2	1.9908 ± 0.0004	-614.7 ± 0.2	-13.2 ± 0.1	-0.1 ± 0.1	+216 ± 2	-7 ± 3	-5 ± 2
T_1 in BaF_2	1.9906 ± 0.0004	-898.7 ± 0.2	-13.6 ± 0.1	-0.1 ± 0.1	+222 ± 2	-4 ± 3	-5 ± 2
T_2 in CaF_2	1.9911 ± 0.0004	-1668.6 ± 0.4	+26.2 ± 0.1	-0.3 ± 0.2	-704 ± 3	+2 ± 4	-3 ± 2
T_2 in SrF_2	1.9914 ± 0.0004	-1815.0 ± 0.4	+22.4 ± 0.1	-0.2 ± 0.2	-575 ± 3	-3 ± 4	-1 ± 2
T_2 in BaF_2	1.9907 ± 0.0004	-1700.4 ± 0.4	+19.8 ± 0.1	-0.1 ± 0.2	-475 ± 3	0 ± 4	-2 ± 2

As indicated in Sec. II, we observed no difference in the ESR properties between the crystals treated with D_2O and H_2O vapor. If a deuterium had replaced a proton in the immediate neighborhood of the Gd^{3+} ion, the resolved superhyperfine structures would have been drastically altered, since the deuteron has a nuclear spin $I=1$ in contrast to that of the proton ($I=\frac{1}{2}$) and a nuclear magnetic moment about $\frac{1}{3}$ the value of the proton. Particularly in the case of the T_1 center, the doublet structure should have been changed radically if an OD^- ion had replaced an OH^- ion. The fact that no change was observed with D_2O treatment justifies eliminating the OH^- ion from the immediate environment of the Gd^{3+} ion.

We now consider the charge-compensation models for the T_1 and T_2 centers involving other important negative ions in the crystal, namely the F^- and O^{2-} ions. If one considers that the charge compensator or compensators are in the first shell, there are four possible combinations of F^- and O^{2-} ions which would achieve charge neutrality: $F^-O_4^{2-}$, $F_3^-O_3^{2-}$, $F_5^-O_2^{2-}$, and $F_7^-O^{2-}$. The combination $F_5^-O_2^{2-}$ can be ruled out immediately, because it cannot give rise to a trigonal symmetry. The combination $F_3^-O_3^{2-}$ is expected to produce at least a four-line (quartet) superhyperfine pattern when \vec{H} is parallel to the $[111]$ direction, which is inconsistent with the observed doublet structure for the T_1 center (see Fig. 5). Thus the $F_3^-O_3^{2-}$ combination can be eliminated for the T_1 center.

The $F_3^-O_3^{2-}$ combination can also be rejected for the T_2 center based on the following considerations. In order to obtain a trigonal symmetry from this combination, only one arrangement of the F^- and O^{2-} ions is possible. The three F^- ions must lie in the same (111) plane and the three O^{2-} ions must lie in the next parallel (111) plane, with the trigonal symmetry axis being perpendicular to these (111) planes. This implies that two of the eight first-shell sites are empty and these sites lie along the symmetry axis. When the magnetic field is applied along the symmetry axis, the three fluorine nuclei become equivalent in that each should give rise to the same superhyperfine splittings. If one considers that the allowed transitions²² are resolved, the resultant superhyperfine pattern would not have a central component, even including the forbidden transitions.²² This is contrary to the observed superhyperfine structure shown in Fig. 6. On the other hand, if the allowed transitions are not resolved, the corresponding structure should contain at most seven components including all the forbidden transitions, which is inconsistent with the large number (at least nine) of component lines contained in the observed structure. Hence, the $F_3^-O_3^{2-}$ model can be ruled out for both the T_1 and T_2 centers.

Comparing the two remaining possibilities, $F^-O_4^{2-}$ and $F_7^-O^{2-}$, it is reasonable to assume that the combination $F^-O_4^{2-}$ is produced after the combination $F_7^-O^{2-}$ during the hydrolysis reaction because of the greater number of substitutional O^{2-} ions involved in the former combination. Since the T_1 center is produced after the T_2 center, the combination $F^-O_4^{2-}$ should be associated with the T_1 center and the combination $F_7^-O^{2-}$ with the T_2 center.

Assuming the above models, it is readily seen that the observed doublet superhyperfine structure for the T_1 center can be explained as arising from the single F^- ion in the $F^-O_4^{2-}$ combination. Furthermore, the linewidth of roughly 2 G observed for each component line in the doublet structure is nearly identical to that of each of the resolved superhyperfine lines in the cubic Gd^{3+} center²² due to the ^{19}F nuclei outside the first shell. If there is more than one ^{19}F nucleus in the first shell, then one would expect to observe either more superhyperfine component lines than two, or broader linewidths for each component line. Thus we conclude that only one magnetic nucleus, namely the ^{19}F , exists in the first shell surrounding the Gd^{3+} ion for the T_1 center. This implies that seven of the eight nearest-neighbor F^- ions have been removed by the hydrolysis treatment and that their role as charge compensators has been taken over by nonmagnetic O^{2-} ions in the $F^-O_4^{2-}$ configuration. This model is illustrated in Fig. 7.

Since the F^- ion in the $F^-O_4^{2-}$ model lies along the trigonal symmetry axis, the superhyperfine interaction with its nucleus requires only two tensor components $T_{||}$ and T_{\perp} . We have found from the doublet splitting with $\vec{H} \parallel [111]$ that $T_{||}$ is approximately 2 G for all three host crystals. On the oth-

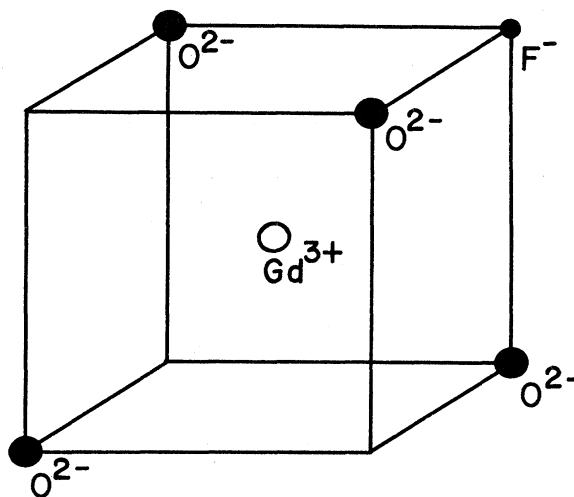


FIG. 7. Charge-compensation structure determined for the T_1 trigonal Gd^{3+} center in alkaline-earth fluorides.

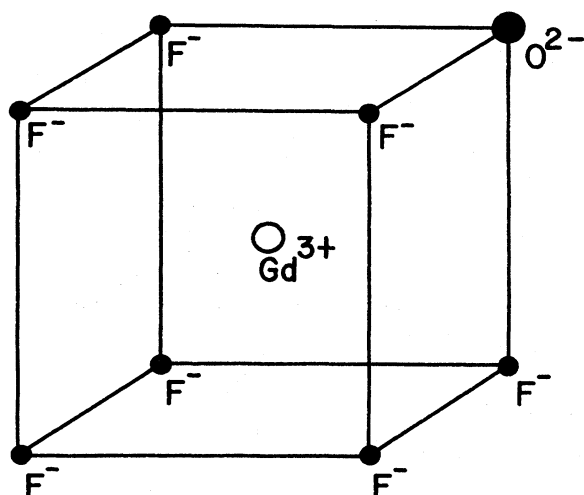


FIG. 8. Charge-compensation structure determined for the T_2 trigonal Gd^{3+} center in alkaline-earth fluorides.

er hand, it was not possible to accurately determine the value of T_1 because of the poor resolution of the doublet splitting when \vec{H} was rotated away from the $[111]$ axis.

One might be tempted to attribute the weak satellite lines observed along with the doublet structure for the T_1 center to forbidden superhyperfine transitions associated with the ^{19}F nuclear spin in the $F^-O_4^{2-}$ configuration. However, such forbidden transitions are not even weakly allowed for \vec{H} parallel to the symmetry axis. It is believed that these weak lines arise from simultaneous spin flips of the Gd^{3+} ion with the distant ^{19}F nuclei which are important for the dynamic nuclear polarization (DNP) of the "solid effect" in the fluorite crystals.²³

To completely characterize the superhyperfine patterns expected for the $F_7O_2^{2-}$ configuration assigned to the T_2 center requires twelve tensor components. The six ^{19}F nuclei not along the trigonal symmetry axis can be grouped into two sets of three equivalent nuclei; each set requires five (three diagonal and two off-diagonal) superhyperfine tensor components.²⁴ The remaining ^{19}F nucleus, since it lies along the symmetry axis, requires only two tensor components. Because of the large number of tensor components involved in the $F_7O_2^{2-}$ configuration, it has not been possible to make a quantitative comparison between the superhyperfine pattern expected for this configuration with the observed superhyperfine pattern. However, there are several factors that mutually reinforce the $F_7O_2^{2-}$ model, namely, the relatively large number of superhyperfine components observed,

the over-all linewidth of each of the unresolved and partially resolved fine-structure lines, and the production sequence of the T_1 and T_2 centers. The $F_7O_2^{2-}$ model is illustrated in Fig. 8.

It should be pointed out that electron-nuclear double-resonance (ENDOR) and ESR studies by other investigators of two trigonal Yb^{3+} and Ce^{3+} centers in heat-treated CaF_2 have provided important guidelines in the construction of the T_1 and T_2 models in the present work. Reddy *et al.*¹⁵ observed two types of trigonal Yb^{3+} centers in CaF_2 by treating the crystals at high temperatures with water vapor containing 11% enriched ^{17}O . One of these trigonal centers, which they denoted by T_2 , occurred before the other type, denoted by T_1 . Based on their ENDOR results, they assigned a $Yb^{3+}-F^-O_4^{2-}$ model for the T_1 center and a $Yb^{3+}-F_7O_2^{2-}$ model for the T_2 center. Subsequently, Chambers¹⁶ reported the observation of two types of trigonal Ce^{3+} ESR centers in treated CaF_2 , which were denoted by A and B according to their sequence of appearance. He suggested that the A and B centers were associated with $Ce^{3+}-F_7O_2^{2-}$ and $Ce^{3+}-F^-O_4^{2-}$ configurations, respectively. He also found that the B -type Ce^{3+} center exhibited a doublet structure for $\vec{H} \parallel [111]$. This structure was concluded to originate from the superhyperfine interaction of the Ce^{3+} ion with the ^{19}F nucleus of the one remaining F^- ion in the first shell.

IV. CONCLUSIONS

A detailed investigation has been made of the T_1 and T_2 trigonal Gd^{3+} ESR centers in single crystals of CaF_2 , SrF_2 , and BaF_2 treated with water vapor at high temperatures. We have successfully produced both the T_1 and T_2 centers in all three alkaline-earth-fluoride crystals. The spin-Hamiltonian constants for the Gd^{3+} centers have been determined by fitting the theoretical spectra obtained from computer diagonalization to the experimental data. A series of heat-treatment experiments has revealed that the T_2 center is always produced before the T_1 center, which is opposite to the sequence previously reported. We have also treated the crystals with D_2O vapor instead of with H_2O vapor, and found no difference in their ESR properties. These results along with the analyses of the superhyperfine structures observed for the T_1 and T_2 centers have enabled us to conclude that the charge-compensation models for the T_1 and T_2 Gd^{3+} centers are similar to those of the two trigonal Yb^{3+} and Ce^{3+} ESR centers observed in treated CaF_2 ; that is, $Gd^{3+}-F^-O_4^{2-}$ for the T_1 Gd^{3+} center and $Gd^{3+}-F_7O_2^{2-}$ for the T_2 Gd^{3+} center.

*Research supported by the National Science Foundation.
 †Based on, in part, work performed by Chi-Chung Yang

in partial fulfillment of the requirements for the degree of Doctor of Philosophy in Physics at Saint Louis Uni-

- versity.
- †Present address: Ames Laboratory, Energy Research and Development Administration, Iowa State University, Ames, IA.
- ¹J. Sierro, *J. Chem. Phys.* **34**, 2183 (1961).
- ²J. Sierro, *Helv. Phys. Acta* **36**, 505 (1963).
- ³C. Ryter and R. Lacroix, *C. R. Acad. Sci. (Paris)* **242**, 2812 (1956).
- ⁴C. Ryter, *Helv. Phys. Acta* **30**, 353 (1957).
- ⁵W. Low, *Phys. Rev.* **109**, 265 (1958).
- ⁶K. Horai, *J. Phys. Soc. Jpn.* **19**, 2241 (1964).
- ⁷T. Rewaj, *Fiz. Tverd. Tela* **10**, 1272 (1968) [*Sov. Phys. - Solid State* **10**, 1014 (1968)].
- ⁸J. M. Baker, B. Bleaney, and W. Hayes, *Proc. R. Soc. A* **247**, 141 (1958).
- ⁹J. Sierro and R. Lacroix, *C. R. Acad. Sci. (Paris)* **250**, 2686 (1960).
- ¹⁰V. M. Vinokurov, M. M. Zaripov, Yu. E. Pol'skii, V. G. Stepanov, G. K. Chirkin, and L. Ya. Shekun, *Fiz. Tverd. Tela* **4**, 2238 (1962) [*Sov. Phys. - Solid State* **4**, 1637 (1963)].
- ¹¹V. M. Vinokurov, M. M. Zaripov, Yu. E. Pol'skii, V. G. Stepanov, G. K. Chirkin, and L. Ya. Shekun, *Fiz. Tverd. Tela* **5**, 2902 (1963) [*Sov. Phys. - Solid State* **5**, 2126 (1964)].
- ¹²J. Sierro, *Phys. Lett.* **4**, 178 (1963).
- ¹³F. Z. Gil'fanov, L. D. Livanova, and A. I. Stolov, *Fiz. Tverd. Tela* **8**, 1165 (1966) [*Sov. Phys. - Solid State* **8**, 929 (1966)].
- ¹⁴A preliminary report of this observation has been made at the 17th Congress AMPERE [A. J. Bevolo and Sook Lee, in *Magnetic Resonance and Related Phenomena, Proceedings of the 17th Congress AMPERE, Finland*, edited by V. Hovi (North-Holland, Amsterdam, 1973), p. 244].
- ¹⁵T. R. Reddy, E. R. Davies, J. M. Baker, D. N. Chambers, R. C. Newman, and B. Ozbay, *Phys. Lett. A* **36**, 231 (1971).
- ¹⁶D. N. Chambers, *Phys. Lett. A* **37**, 77 (1971).
- ¹⁷Sook Lee, Chi-Chung Yang, and Albert J. Bevolo, *Phys. Rev. B* **10**, 4515 (1974).
- ¹⁸A. A. Antipin and I. N. Kurkin, *Fiz. Tverd. Tela* **6**, 947 (1964) [*Sov. Phys. - Solid State* **6**, 730 (1964)].
- ¹⁹L. A. Boatner, R. W. Reynolds, and M. M. Abraham, *J. Chem. Phys.* **52**, 1248 (1970).
- ²⁰J. E. Drumheller, *J. Chem. Phys.* **38**, 970 (1963).
- ²¹V. M. Vinokurov, M. M. Zaripov, Yu. E. Pol'skii, V. G. Stepanov, G. K. Chirkin, and L. Ya. Shekun, *Fiz. Tverd. Tela* **5**, 599 (1963) [*Sov. Phys. - Solid State* **5**, 436 (1963)].
- ²²Sook Lee, Albert J. Bevolo, and Chi-Chung Yang, *J. Chem. Phys.* **60**, 1628 (1974).
- ²³Sook Lee, V. P. Jacobsmeyer, and T. V. Hynes, *Phys. Rev. Lett.* **17**, 536 (1966).
- ²⁴J. M. Baker, E. R. Davies, and J. P. Hurrell, *Proc. R. Soc. A* **308**, 403 (1968).